Accessible Mandelbrot Sets in the Family $z^n + \lambda/z^n$ *

March 31, 2015

*2000 MSC number: Primary 37F10; Secondary 37F45

0 Introduction

In recent years, there have been a number of papers [1], [14] dealing with the topology of Julia sets that arise from parameters lying in certain Mandelbrot sets that are subsets of the parameter plane for the family of rational maps given by

$$F_\lambda(z) = z^n + \frac{\lambda}{z^n}$$

where $n \geq 2$. In Figure 1 we display the parameter plane for this family when $n = 3$ and 4. Note that there are two large copies of the Mandelbrot set visible in this picture when $n = 3$ and three when $n = 4$; these are known as the "principal" Mandelbrot sets. But there are many other smaller copies of "baby" Mandelbrot sets in these parameter planes as well, as it is known [16] that they are dense in the bifurcation locus for a holomorphic family of rational maps.

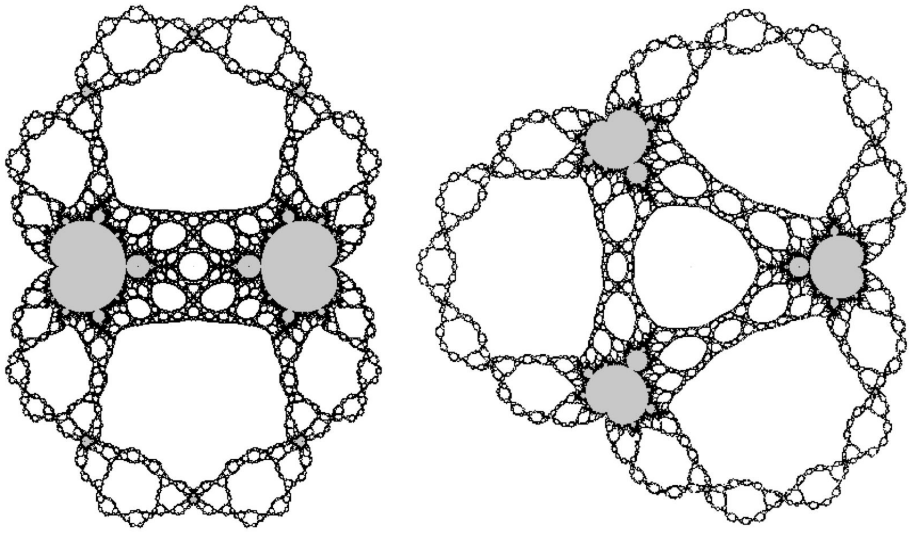

Figure 1: The parameter planes when $n = 3$ (left) and $n = 4$ with the principal Mandelbrot sets in grey.

In these parameter planes, the external region consists of parameters for which the corrresponding Julia sets are Cantor sets. There is also a small disk centered at the origin in which the corresponding Julia sets are Cantor sets of simple closed curves [15]. This is the McMullen domain. In the remaining region, the Julia sets are always connected sets. This region is therefore called the connectedness locus; it is known that this set is a connected set in the parameter plane [10].

In Figure 2 we display the parameter plane for this family when $n = 2$ together with several magnifications. In this image, there is a large main cardioid in what appears to be a principal Mandelbrot set in this image that extends to the external boundary of this set. In the magnifications, there appear to be other baby Mandelbrot sets that extend out to the boundary (we call these "accessible" Mandelbrot sets), as well as other baby Mandelbrot sets that do not extend to the boundary (these are "buried" Mandelbrot sets).

The topology of the Julia sets drawn from these Mandelbrot sets is quite interesting. It is known that, for a given value of n, all of the Julia sets drawn from the main cardioids of the principal Mandelbrot sets are the same topologically, i.e., they are all homeomorphic to one another [1]. These sets are called "checkerboard" Julia sets. But for other accessible main cardioids, the topology of the Julia sets is quite different and only those cardioids that are symmetric under certain rotations or complex conjugation are homeomorphic [14].

For the buried Mandelbrot sets, the situation is again very different: all Julia sets drawn from such a main cardioid are Sierpiński curves (i.e., they are homeomorphic to the well-known Sierpiński carpet fractal) and hence they all have the same topology [9].

It is known that there are exactly $n - 1$ principal Mandelbrot sets in

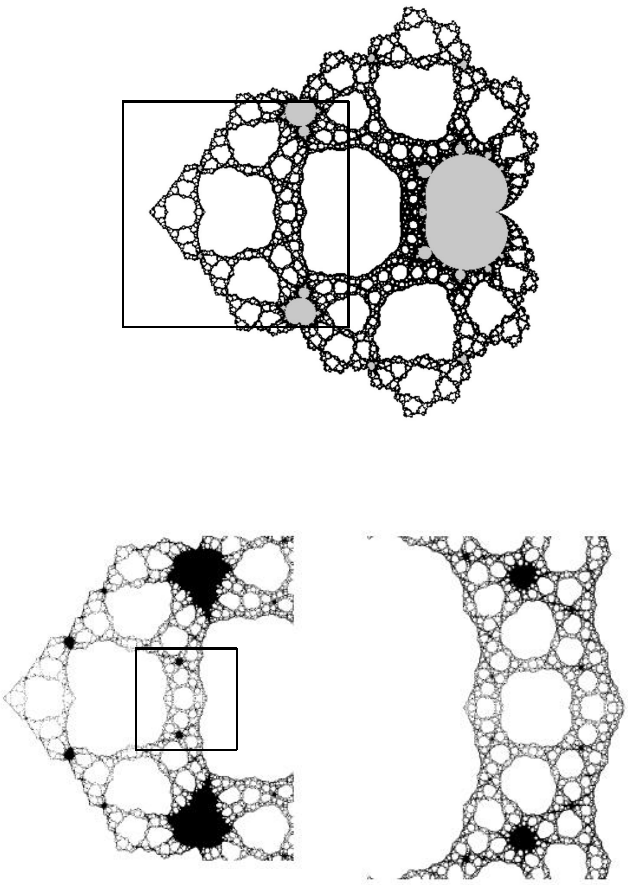

Figure 2: The parameter plane for the family $z^2 + \lambda/z^2$ together with two magnifications.

the parameter plane for the maps $z^n + \lambda/z^n$ [4]. These are the Mandelbrot sets which have base period one (defined below). It is also known that there are infinitely many other accessible Mandelbrot sets when $n \geq 3$ [5] and also when $n = 2$ [8]. And finally, infinitely many buried Mandelbrot sets have been shown to exist [11]. However, to date there has been no complete description of the arrangement of these Mandelbrot sets in these parameter planes.

Our goal in this paper is to describe the exact arrangement of all of the accessible Mandelbrot sets in these families. We shall show that there is a unique accessible Mandelbrot set whose cusp is at the landing point of each external ray in the parameter plane that is periodic under the map $\theta \mapsto n\theta$. This provides the complete classification of all of these accessible Mandelbrot sets.

1 Preliminaries

Consider the family of rational maps given by

$$F_\lambda(z) = z^n + \frac{\lambda}{z^n}$$

where $n \geq 2$. One checks easily that the point at ∞ is a superattracting fixed point for these maps. Hence there is an immediate basin of attraction of ∞ which we denote by B_λ. There is also a neighborhood of 0 that is mapped into this basin. This neighborhood may or may not be disjoint from B_λ. In this paper, we shall consider only the case where the preimage of B_λ containing 0 is disjoint from B_λ. In this case we call this preimage the trap door and denote it by T_λ. The full basin of ∞ is then the union of the infinitely many distinct preimages of B_λ.

The Julia set of F_λ, denoted by $J(F_\lambda)$, has several definitions. First, $J(F_\lambda)$ is the closure of the set of repelling periodic points of F_λ. Second,

$J(F_\lambda)$ is also the set of points at which the family of iterates of F_λ fails to be a normal family in the sense of Montel. And third, just as in the case of polynomials, $J(F_\lambda)$ is also the boundary of the full basin of ∞.

There are several symmetries associated with this family of maps. First, let ω be a primitive $2n^{\text{th}}$ root of unity. Then we have $F_\lambda(\omega z) = -F_\lambda(z)$. So, if n is even, $F_\lambda^2(z) = F_\lambda^2(\omega^j z)$ for each j, so the orbits of these points are eventually the same. If n is odd, we have $F_\lambda(-z) = -F_\lambda(z)$ and so the orbits of z and ωz behave symmetrically under $z \mapsto -z$. In either case, it follows that $J(F_\lambda)$, B_λ, and T_λ are all symmetric under $z \mapsto \omega z$, i.e., we have $2n$-fold symmetry in the dynamical plane.

Let H_λ be the involution $H_\lambda(z) = \lambda^{1/n}/z$. Then $F_\lambda(H_\lambda(z)) = F_\lambda(z)$ so $J(F_\lambda)$ is also symmetric under H_λ. Note that H_λ interchanges B_λ and T_λ.

There are $2n$ "free" critical points for F_λ given by $\lambda^{1/2n}$. We denote these critical points by $c_0, \ldots, c_{2n-1}$, where $0 \leq \operatorname{Arg} c_0 < \pi/n$ and the other c_j are ordered in the counterclockwise direction. We call these critical points free because there are two other critical points: one at ∞, which is fixed, and the other at 0, which is mapped directly to ∞. So these two critical points are not "free." There are only 2 critical values corresponding to the free critical points of F_λ given by $v_\lambda = \pm 2\sqrt{\lambda}$; n of the free critical points are mapped to $+v_\lambda$ and the other n are mapped to $-v_\lambda$. However, there really is only one critical orbit up to symmetry, since, when n is even, both $\pm v_\lambda$ are mapped onto the same point, whereas, when n is odd, the orbits of $\pm v_\lambda$ behave symmetrically under $z \mapsto -z$. There are also $2n$ prepoles for F_λ given by $(-\lambda)^{1/2n}$. Note that all of the critical points and prepoles lie on the same circle which we call the *critical circle*. Also, each involution H_λ fixes two critical points c_j and c_{j+n}.

The difference between the behaviors of the critical orbits when n is even or odd causes a slight difference in the periods associated to parameters

drawn from the main cardioids of the Mandelbrot sets that we will work with. Let λ be the center of the main cardioid of such a Mandelbrot set (i.e., λ is the unique parameter in that region for which a critical orbit is periodic). Suppose that c_j is a critical point that lies on this periodic orbit and that $F_\lambda^k(c_j)$ is the first subsequent critical point on the orbit of c_j. Then, if n is even, we must have that $F_\lambda^k(c_j) = c_j$ since all the critical orbits agree at iteration two and beyond. However, if n is odd, there is a second possible scenario. It could be the case that, when the orbit of c_j lands on a critical point at iteration k, this orbit now lands on $-c_j$. This follows from the fact that the orbits of any pair of critical points c_k and $-c_k$ are symmetric under the $z \mapsto -z$ symmetry. So these orbits are either distinct or else they are the same. In either case, all of the other critical points must land on these orbits. So, if we have that $F_\lambda^k(c_j) = -c_j$, then the period of c_j (and $-c_j$) is $2k$, not k. In any event, we say in both cases that such a Mandelbrot set has *base period* k if some critical orbit first returns to the critical circle at iteration k. For example, in the parameter plane for $n = 3$ displayed in Figure 1, both principal Mandelbrot sets have base period 1. The right-hand Mandelbrot set does have a parameter at the center of the main cardioid for which there is a superattracting fixed point. However, the left-hand principal Mandelbrot set has a parameter at the center of the main cardioid for which two critical points are interchanged as above by F_λ, so we have an attracting cycle of period two. However, by definition, this set has base period one.

Throughout this paper we shall assume that the orbits of the critical points are all bounded. In this case it is known that $J(F_\lambda)$ is always a connected set [10], [12].

The straight rays extending out from the origin and passing through the critical points are called the critical point rays. These are mapped by F_λ two-to-one onto the critical value rays given by tv_λ where $t \geq 1$. Let S_j

denote the open sector bounded by the two critical point rays through c_{j-1} and c_j. Then each S_j is mapped one-to-one onto the complement of the two critical value rays. It is known that the set of points in $J(F_\lambda)$ whose orbits remain for all iterations in the two sectors $S_0 \cup S_n$ is a Cantor set on which F_λ is conjugate to the one-sided shift map on two symbols. Call this Cantor set Λ. Then Λ meets ∂B_λ in two points, both of which are fixed when n is odd, and one is fixed and the other pre-fixed when n is even. This follows since the external ray of angle 0 is clearly contained in the sector S_0, and this ray lands on a fixed point in ∂B_λ, while the external ray of angle $1/2$ lies in S_n and lands on a different fixed point if n is odd or on a pre-fixed point if n is even. We denote the fixed point that lies in Λ and in the right half-plane by p_λ. By the $z \mapsto -z$ symmetry, the other point in $\partial B_\lambda \cap \Lambda$ is $-p_\lambda$. Similarly, there is a pair of points $\pm q_\lambda$ lying in $\partial T_\lambda \cap \Lambda$. We choose q_λ to be the point that lies in the sector S_0 so that $-q_\lambda$ lies in the sector S_n. See [6].

The set of points that lie in Λ, T_λ, and all of the preimages of T_λ whose boundaries meet Λ in a pair of points forms what is known as a *Cantor necklace*. This set is defined as follows. Consider the Cantor middle-thirds set lying in the interval $[0, 1]$ on the x-axis in the plane. Adjoin to this set an open disk in place of each removed open interval so that the boundary of this disk meets the Cantor set at the two endpoints of this removed open interval. This is the Cantor middle-thirds necklace. Then any planar set that is the image of this necklace under a map that is continuous, one-to-one, and onto is called a Cantor necklace.

2 Internal Rays in the Dynamical Plane

In order to prove the existence of the accessible Mandelbrot sets in the parameter plane, we first need to introduce the notion of internal rays in the dynamical plane. For simplicity, for most of this paper, we shall restrict to the case where $n = 2$, i.e., to the family of maps

$$F_\lambda(z) = z^2 + \frac{\lambda}{z^2}.$$

We describe the minor modifications necessary for the case $n > 2$ at the end of this paper.

As mentioned above, we shall assume throughout this paper that the critical values do not lie in B_λ or T_λ (and so $J(F_\lambda)$ is connected). As is well known [10], in this case, B_λ is simply connected and there is a natural uniformization of B_λ that conjugates $F_\lambda \,|\, B_\lambda$ to $z \mapsto z^2$ on the open unit disk. The external ray of angle θ, denoted by $\xi_\theta^\lambda = \xi_\theta$, is the curve that maps to the straight ray of angle θ under this conjugacy. All rational rays are known to land at a unique point in ∂B_λ [18], so the external ray of angle 0 lands at the fixed point p_λ and $\xi_{1/2}$ lands at $-p_\lambda$. Since $H_\lambda(T_\lambda) = B_\lambda$, this uniformization may then be extended to T_λ. We then assign angles to the corresponding rays so that the trap door ray of angle 0 in T_λ, namely $\tau_0^\lambda = \tau_0$, now extends from the origin to q_λ, while $\tau_{1/2}$ extends from 0 to $-q_\lambda$. Therefore $F_\lambda(\tau_0) = F_\lambda(\tau_{1/2}) = \xi_{1/2}$. We then have the corresponding trap door rays τ_θ lying in T_λ, where the angles θ are chosen so that they increase in the counterclockwise direction around the origin. (Note that $H_\lambda(\xi_\theta) \neq \tau_\theta$ if $\theta \neq 0, 1/2$.)

We now define the internal rays of angles 0 and $1/2$ for F_λ. These will be curves that pass through portions of the Julia set and certain preimages of B_λ and connect the endpoints of the corresponding external ray in ∂B_λ to the endpoints of the corresponding trap door ray in ∂T_λ. We may successively

pull back the trap door rays τ_0 and $\tau_{1/2}$ to each of the preimages of T_λ that lie in the Cantor necklace in $S_0 \cup S_2$. These preimage curves each connect to two distinct points in the invariant Cantor set Λ. Then, as shown in [6], the union of these curves that lie in the sector S_0 together with the portion of Λ in this region is a continuous curve that connects p_λ to q_λ. This is the internal ray which we denote by ν_0. The internal ray $\nu_{1/2}$ is defined in similar fashion in the opposite sector $-S_0$, so, by the $z \mapsto -z$ symmetry, $\nu_{1/2} = -\nu_0$. Note that each of these internal rays contains a unique preimage of 0. The full ray of angle 0 (resp., 1/2) is then the union of the internal, external, and trap door rays of angles 0 (resp., 1/2). Then one checks easily that the full ray of angle 0 is mapped one-to-one onto the pair of full rays of angles 0 and 1/2 together with the origin. The full ray of angle 1/2 is mapped in similar fashion onto the same full rays and the origin.

We next define the internal rays of angle $j/2^k$ for F_λ where $k \geq 2$. These will be extensions of the external rays $\xi_{j/2^k}$ into the complement of $B_\lambda \cup T_\lambda$. We will define these internal rays inductively by simply taking the particular preimages of the internal rays $j/2^{k-1}$ that meet ∂B_λ. To begin, we define the internal rays $\nu^\lambda_{1/4} = \nu_{1/4}$ and $\nu_{3/4}$ to be the two other curves contained in the complement of $B_\lambda \cup T_\lambda$ that are each mapped one-to-one over $\nu_0 \cup \nu_{1/2}$ as well as $\tau_0 \cup \tau_{1/2}$ and the origin. Specifically, $\nu_{1/4}$ is given by $i\nu_0$ and $\nu_{3/4} = -\nu_{1/4}$, so $\nu_{1/4}$ (resp., $\nu_{3/4}$) lies in the upper (resp., lower) half-plane. As above, both $\nu_{1/4}$ and $\nu_{3/4}$ meet ∂B_λ and ∂T_λ at unique points. See Figure 3. We then define the full rays of angles 1/4 and 3/4 to be the union of the corresponding internal, external, and trap door rays with this angle. This gives a continuous curve extending from the origin to ∞. These full rays are also mapped one-to-one over the union of full rays of angles 0 and 1/2 as well as the origin.

Now consider the open region in the complement of $\overline{B}_\lambda \cup \overline{T}_\lambda$. The four internal rays $\nu_0, \nu_{1/4}, \nu_{1/2}$, and $\nu_{3/4}$ divide this region into four open sectors

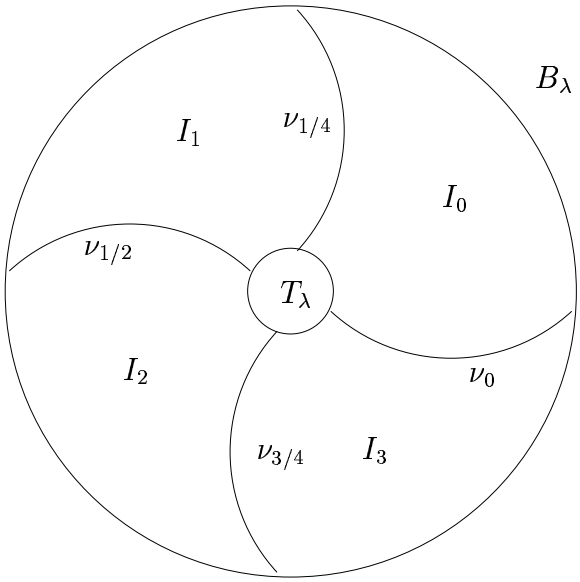

Figure 3: The internal rays of angles 0, 1/4, 1/2, and 3/4.

$I_0, \ldots, I_3$ where I_0 is bounded by ν_0, $\nu_{1/4}$, and portions of ∂B_λ and ∂T_λ, and the other three sectors are arranged in the counterclockwise direction. Note that F_λ maps I_0 and I_2 two-to-one over $I_0 \cup I_1 \cup \nu_{1/4}$ as well as the portion of T_λ lying above $\tau_0 \cup \tau_{1/2}$ and, similarly, I_1 and I_3 are mapped two-to-one over $I_2 \cup I_3 \cup \nu_{3/4}$ plus the portion of T_λ lying below $\tau_0 \cup \tau_{1/2}$. In addition, the critical point c_j lies in I_j for each j.

We may then define the itinerary $S(z)$ of any point z whose orbit remains for all iterations in the union of the I_j in the usual way: $S(z) = (s_0 s_1 s_2 \ldots)$ if $F_\lambda^j(z) \in I_{s_j}$. Note that, in such an itinerary, 0 and 2 can only be followed by 0 or 1 because of how the corresponding sectors are mapped. Similarly, 1 and 3 can only be followed by 2 or 3. Any finite or infinite sequence that follows this coding is called an allowable itinerary.

For the moment we assume that the critical orbits never land on the internal or trap door rays of angles 0 and 1/2. Hence each critical point c_j whose orbit is bounded in $\mathbb{C}$ has an infinite itinerary of the form $(s_0 s_1 s_2 \ldots)$. Moreover, since all the critical points land on the same point after two iterations, the "tail" of the itinerary of each critical point, namely $(s_2 s_3 s_4 \ldots)$, is the same.

Since F_λ maps I_0 two-to-one over $I_0 \cup I_1 \cup \nu_{1/4}$ plus a portion of T_λ and, by assumption, the critical value does not lie on the internal or trap door ray of angle 1/4, it follows that there are two preimages of $\nu_{1/4}$ in I_0. We call these preimages the boundary curves. One of these boundary curves must extend from ∂B_λ to one of the two preimages of ∂T_λ that lie on the bounding internal rays of I_0 and the other necessarily extends from ∂T_λ to the opposite preimage of ∂T_λ. This follows since these two curves are located symmetrically with respect to the involution $H_\lambda(z) = \lambda^{1/2}/z$ that fixes the critical point c_0. This implies that there are then two possibilities for how these boundary curves are arranged as shown in Figure 4. These two different cases depend upon whether $F_\lambda(c_0) \in I_0$ or $F_\lambda(c_0) \in I_1$, both of which may occur.

We now append the preimages of the trap door ray $\tau_{1/4}$ to these two curves so that each of these longer boundary curves now extends to one of the first preimages of 0. These two curves then divide I_0 into three separate regions. We call the unique boundary curve that meets the boundary of B_λ the internal ray of angle 1/8, so $\nu_{1/8}$ extends from ∂B_λ to a first preimage of 0. If $F_\lambda(c_0)$ lies in I_0, then there is an open region that connects ∂B_λ to ∂T_λ which is mapped two-to-one onto I_0. This is the "connecting" region I_{00}. One checks easily that this occurs when $\operatorname{Im} \lambda > 0$. There are also two other open subsets in I_0 that are mapped one-to-one onto I_1. Neither of these sets connects ∂B_λ to ∂T_λ; rather, one abuts ∂B_λ (we call this the "non-

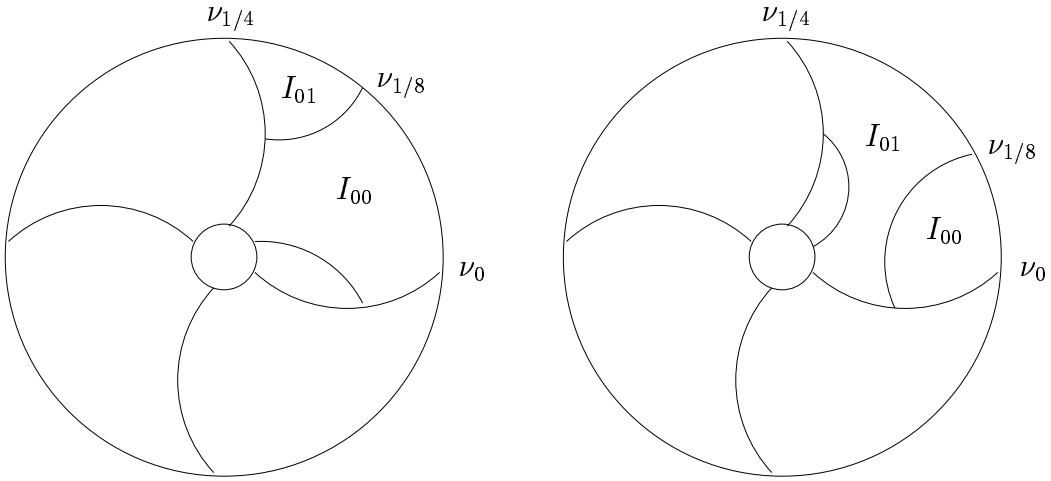

Figure 4: The two possible configurations for $\nu_{1/8}$. The unmarked curves are also boundary curves that are mapped to $\nu_{1/4}$.

connecting" region I_{01}) and the other abuts ∂T_λ. Note that, in this case, the internal ray $\nu_{1/8}$ extends from ∂B_λ to the "middle" of $\nu_{1/4}$, i.e., to the unique first preimage of 0 in this ray. On the other hand, if the image of c_0 lies in I_1 (which occurs if $\operatorname{Im}\lambda < 0$), there is now a connecting region I_{01} that is mapped two-to-one onto I_1 and a pair of other regions mapped one-to-one to I_0. The internal ray $\nu_{1/8}$ now extends from ∂B_λ to the middle of ν_0 and the non-connecting region bounded by this ray is called I_{00}. In particular, we have that there is an open set of parameters for which a critical value lies in I_j.

By the fourfold symmetry, we have a similar configuration in the other regions I_j and thus we can define the internal rays $\nu_{3/8}, \nu_{5/8}$, and $\nu_{7/8}$. See Figure 5.

To summarize, at this first stage, each of the regions I_{s_0} may be divided into three separate subregions. Exactly two of these subregions abut ∂B_λ.

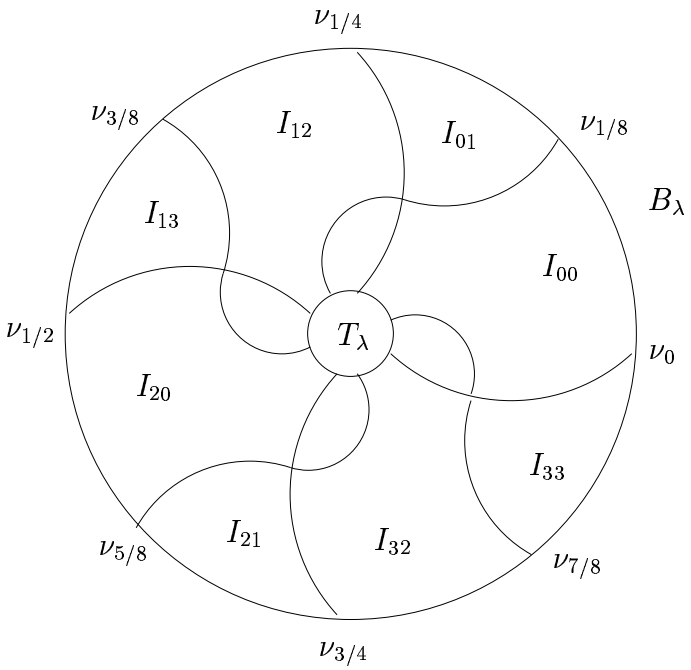

Figure 5: The $j/8$ internal rays when c_0 lies in I_{00} together with the connecting and non-connecting regions in this case.

We denote these special regions by $I_{s_0 s_1}$ where there are two possibilities for the digit s_1. One of these regions is a non-connecting region that is mapped one-to-one onto its image I_{s_1} while the other is the connecting region that is mapped two-to-one onto its image. The corresponding internal ray $\nu_{j/8}$ provides a portion of the boundary of these two regions. And there is an open set of parameters for which the critical point in I_{s_0} lies in either possible connecting region. These are the open sets that we shall use in a later section to define the polynomial-like maps that will generate the accessible Mandelbrot sets. We will not consider the third region in I_{s_0} as this region will not play a role when we generate these Mandelbrot sets. See Figure 5 for a picture of the arrangement of the regions $I_{s_0 s_1}$ in the case where $F_\lambda(c_0) \in I_0$.

As a remark, if the critical value does lie in $\nu_{1/4}$, then the connecting

region becomes a pair of open disks whose boundaries meet at exactly one point, namely the critical point that lies on their boundary. One of these disks extends to ∂B_λ, the other to ∂T_λ.

We may now continue with this procedure. We begin by assuming that the critical values lie in one of the two regions that abut ∂B_λ, not in the third region that does not extend out to ∂B_λ. This is possible since, as λ rotates around a simple closed curve surrounding the origin, the critical values both rotate half way around a similar simple closed curve. Hence we may choose this curve in the parameter plane so that the critical values rotate around in a narrow annular neighborhood bounded on the outside by ∂B_λ. Consequently a critical value enters each region $I_{s_1 s_2}$, and thus there is an open set of parameters for which this occurs.

First, in the non-connecting region $I_{s_0 s_1}$ that is mapped one-to-one onto I_{s_1}, we can simply pull back the boundary curves that we previously constructed in I_{s_1} via F_λ^{-1}. The preimage of $\nu_{j/8}$ in I_{s_1} then gives a curve that connects ∂B_λ to one of the second preimages of 0 lying in the boundary of $I_{s_0 s_1}$. As before, there are two such second preimages of 0 in this region, but which one the preimage of $\nu_{j/8}$ connects to is already determined since F_λ is one-to-one in this region. This defines the internal ray $\nu_{j/16}$ or $\nu_{(j+8)/16}$ that lies in $I_{s_0 s_1}$. Note that this now gives two smaller non-connecting regions $I_{s_0 s_1 s_2}$ that abut ∂B_λ.

In the second case, $I_{s_0 s_1}$ is now a connecting region and hence contains a critical point. Therefore this region now divides into five subregions. The reason for this is that, since F_λ maps $I_{s_0 s_1}$ two-to-one onto I_{s_1} and there are two preimages of $\nu_{1/4}$ in I_{s_1}, there must now be four preimages of these two curves in $I_{s_0 s_1}$ and hence this divides this region into five subregions. Four of these subregions are mapped one-to-one onto their images and one subregion (containing the critical point) is mapped two-to-one onto its image.

However, only two of these regions meet ∂B_λ. By assumption, one of these abutting regions must contain the critical point and this region therefore extends to ∂T_λ (this is the connecting region at this stage); the other as before is mapped one-to-one onto its image (this is the non-connecting region) and the new internal ray is defined to be the curve that separates these two regions. There are also three additional preimage regions, each of which is mapped one-to-one onto its image in $I_{s_1 s_2}$. However, none of these regions meet ∂B_λ, so these sets again will not play a role in the polynomial-like map construction in the next section. Note also that a critical value may now lie in any of the four regions abutting ∂B_λ.

We now continue inductively. At the k^{th} stage, we simply pull back all of the internal rays of angle $j/2^{k+1}$ together with the other previously defined boundary curves. In the sector I_{s_0}, these curves then bound exactly 2^k open disks that meet ∂B_λ and are given by $I_{s_0 \ldots s_k}$. Here, s_0 is fixed, and $s_1 \ldots s_k$ can be any of the allowable sequences of length k that can follow s_0. Each of these is bounded by a pair of portions of internal rays of angles $j/2^{k+2}$ and $(j+1)/2^{k+2}$ that meet ∂B_λ, by the portion of ∂B_λ between these two rays, and by other curves that are portions of the earlier defined boundary curves or their preimages (and, in one special case, by a portion of ∂T_λ). As earlier, $2^k - 1$ of these disks that abut ∂B_λ do not extend down to ∂T_λ and so are the non-connecting regions. None of these disks contain the critical point c_{s_0}, and so each is mapped one-to-one onto $I_{s_1 \ldots s_k}$. Therefore we can pull back the internal ray structure already constructed in the set $I_{s_1 \ldots s_k}$ to determine how the external rays of angle $j/2^{k+3}$ as well as the other boundary curves are configured in these preimages. More specifically, we have two regions in $I_{s_1 \ldots s_k}$ that meet ∂B_λ, namely $I_{s_1 \ldots s_k s_{k+1}}$ where there are two choices for the digit s_{k+1}. These regions are separated in an already determined fashion by the previously defined boundary curves, and so their preimages in $I_{s_0 \ldots s_k}$

given by $I_{s_0 \ldots s_{k+1}}$ have a similar configuration. As above, there are parameters where a critical value lies in any of these regions.

The one exception to this is again the open disk that is the connecting region. This disk contains the critical point and extends down to ∂T_λ. Suppose this region is $I_{s_0 \ldots s_k}$. Then F_λ maps this region two-to-one onto its image $I_{s_1 \ldots s_k}$, so the two subregions $I_{s_1 \ldots s_n s_{k+1}}$ touching ∂B_λ may have one or two preimages in $I_{s_0 \ldots s_k}$ depending upon the location of the critical value in these regions. As above, the critical value can lie in either of these regions. So, depending upon the location of this critical value, we can determine how the new external ray that separates these preimages in $I_{s_0 \ldots s_k}$ is configured, i.e., to which of the k^{th} preimages of 0 it connects. In any event, we have that F_λ maps one of these preimages two-to-one onto its image and this gives the new connecting region at this stage. Thus we have the following results:

Proposition 1. *Given an allowable sequence $s_0 \ldots s_k$, there are parameter values for which there is an open set $I_{s_0 \ldots s_k}$ that contains the critical point c_{s_0} and is mapped two-to-one onto its image. This is the connecting region that extends from ∂B_λ to ∂T_λ. As a consequence, there also exists an open set in the parameter plane for which a critical value lies in $I_{s_1 \ldots s_k}$ for any allowable sequence of the form $s_1 \ldots s_k$.*

For the polynomial-like maps that we will consider in the next section, the connecting regions whose boundaries meet the internal ray of angle 0 or 1/2 will play an important role. As the following proposition shows, there are relatively few such connecting regions.

Proposition 2. *The only connecting regions whose boundary meets the internal ray of angles 0 or 1/2 are $I_{0 \ldots 0}$, $I_{3 \ldots 3}$, and each of their three symmetrically located regions under the fourfold symmetry.*

Proof: Consider the region I_0. As we showed above, each of the two con-

necting regions I_{00} and I_{01} in this region meet the internal ray of angle 0 (see Figure 4). Note that the connecting region I_{01} is the rotation of another connecting region I_{33} via $z \mapsto iz$. Using the inductive procedure described above, I_{00} can be broken into two different connecting regions, I_{000} and I_{001}. The internal ray 1/16 determines this structure. For I_{000}, this ray meets the internal ray of angle 1/8 and hence this region has a portion of its boundary on the internal ray of angle 0. In the other case, the 1/16 internal ray now connects to the boundary curve of a region that does not meet B_λ, and so the boundary of I_{001} does not meet the internal ray of angle 0. A similar argument using the internal ray of angle 3/16 shows that the connecting region I_{013} meets the internal ray of angle 0, while the connecting region I_{012} does not. Hence any of the connecting regions of the form $I_{001s_3\ldots s_k}$ or $I_{012s_3\ldots s_k}$ do not meet this internal ray.

Continuing in this fashion, we use the internal rays of angles 1/32 and 7/32 to show that the boundaries of the connecting regions I_{0000} and I_{0133} meet the internal ray of angle 0. Continuing inductively shows that the only connecting regions in I_0 whose boundaries meet the internal ray of angle 0 are those of the form $I_{0\ldots0}$ and $I_{013\ldots3}$ (where I_{01} is also included in this list). Then the $z \mapsto iz$ symmetry gives the result.

□

3 Polynomial-like Mappings

Our goal in this section is to prove the existence of infinitely many accessible Mandelbrot sets in the parameter plane for the family F_λ, one corresponding to each external ray whose angle is periodic under angle-doubling. To accomplish this, we make use of the concept of polynomial-like maps [2], [13]. Recall that a family of holomorphic maps G_λ is said to be polynomial-like of

degree two if

1. The parameter λ lies in a closed disk $\mathcal{O}$ in the complex plane and G_λ depends analytically on λ;

2. For each λ there are open disks $U_\lambda \subset V_\lambda$ that depend continuously on λ and G_λ maps U_λ two-to-one onto V_λ, so there is a unique critical point $c_\lambda \in U_\lambda$ and critical value $v_\lambda \in V_\lambda$;

3. As λ rotates once around the boundary of $\mathcal{O}$, the critical value lies in $V_\lambda - U_\lambda$ and rotates once around U_λ.

For such a family of maps, it is then known that there is a copy of the Mandelbrot set in $\mathcal{O}$ and, for λ-values in this set, there is a subset of U_λ on which G_λ is conjugate to the corresponding quadratic map.

The open disks U_λ that we shall use for this construction will be slight variations of the connecting and non-connecting sets $I_{s_0 \ldots s_k}$ described in the previous section.

Consider the connecting region $I_{s_0 \ldots s_k}$. We may expand this region slightly by including a portion of B_λ and T_λ in this set. To accomplish this, first assume that the portion of the boundary of this region reaching out to ∂B_λ is given by the two internal rays $j/2^{k+2}$ and $(j+1)/2^{k+2}$. Then we may extend this region slightly into B_λ by first choosing a specific level set given by the Böttcher coordinate on B_λ, and then adding to $I_{s_0 \ldots s_k}$ the adjacent "rectangular" region in B_λ bounded by this level set and the two external rays with the above angles $j/2^{k+2}$ and $(j+1)/2^{k+2}$. Via the H_λ symmetry, we can add a similar rectangular region in T_λ to this set. For simplicity, we also call this expanded region $I_{s_0 \ldots s_k}$.

Since $I_{s_0 \ldots s_k}$ is a connecting region, this set is mapped two-to-one onto an expanded region that we also call $I_{s_1 \ldots s_k}$. Here the outer boundary of this

set again includes a rectangular region in B_λ (and possibly but not always in T_λ), this time extending a bit further toward ∞ since the level set of the Böttcher coordinate is mapped further outward. Continuing in this fashion, we let $I_{s_j \dots s_k}$ be the images of $I_{s_{j-1} \dots s_k}$.

We now show that there is an open disk of parameters for which a critical value lies in any given (connecting or non-connecting) region $I_{s_0 \dots s_k}$. Because the parameter plane is symmetric under complex conjugation (F_λ is conjugate to $F_{\overline{\lambda}}$ via $z \mapsto \overline{z}$), it suffices to consider parameters in the upper half-plane. Then one checks easily that this implies that $F_\lambda(c_0)$ lies in I_0, so the itinerary of c_0 begins with 00. In fact, as shown in [3], it is precisely when $\lambda \in \mathbb{R}^-$ that the critical value v_λ in the upper half-plane lies on the internal ray of angle 1/4.

We shall also assume that the itinerary under consideration is not $00 \dots 0$. The reason for this is that it is well known that there is no accessible Mandelbrot set corresponding to the itinerary $(\overline{0})$. Indeed, the tip of the "tail" of the set of parameters with this itinerary (i.e., the map that should be conjugate to $z^2 - 2$) now lies at the origin in the parameter plane, and the map z^2 does not correspond to the parameter that would lie at this point in a Mandelbrot set. On the other hand, for $n \geq 3$, it is known [4] that there is a "principal" Mandelbrot set lying along the positive real axis in the parameter plane corresponding to this itinerary.

Proposition 3. *Suppose $I_{s_0 \dots s_k}$ is a connecting region which therefore contains the critical point c_{s_0}. Let $\mathcal{O}$ be the set of parameters for which $F_\lambda(c_{s_0})$ lies in $I_{s_1 s_2 \dots s_k}$. Then $\mathcal{O}$ is an open disk, and, as λ winds around the boundary of $\mathcal{O}$, the critical value $F_\lambda(c_{s_0})$ winds once around the boundary of $I_{s_1 s_2 \dots s_k}$.*

Proof: As above, we may assume that this connecting region is $I_{00 s_2 \dots s_k}$ which thus contains c_0. The result for the other connecting regions follows by symmetry. By our earlier results we know that there is a non-empty

open set of parameters for which $F_\lambda(c_0)$ lies in the open region $I_{0s_2\ldots s_k}$. By construction, on the boundary of this set of parameters, the corresponding critical value lies in the boundary of $I_{0s_2\ldots s_k}$.

To prove that $\mathcal{O}$ is an open disk, we first choose a natural parameterization $\beta_\lambda(\theta)$ of the portion of the boundary of $I_{0s_2\ldots s_k}$ that lies in the chosen level set given by the Böttcher coordinate in B_λ. We may choose this parametrization so that, for a fixed θ, the point $\beta_\lambda(\theta)$ varies analytically with λ. Then standard results from complex dynamics show that there is a unique parameter λ_θ for which v_{λ_θ} lies on the given point $\beta_{\lambda_\theta}(\theta)$, i.e., for this unique parameter, the critical value lies on that one special boundary point of $I_{0s_2\ldots s_k}$. Hence we have a unique portion of $\partial\mathcal{O}$ for which the critical values of these maps lie in the portion of the boundary of $I_{0s_2\ldots s_k}$ given by the Böttcher coordinate in B_λ. As λ varies continuously along $\partial\mathcal{O}$, v_λ also moves continuously around the boundary of the corresponding region in the dynamical plane. Hence there can be at most one boundary component of $\mathcal{O}$, and, because of the uniqueness of the parameters for which v_λ lies along the level set in B_λ, it follows that as λ winds around $\partial\mathcal{O}$, v_λ winds once around $\partial I_{0s_2\ldots s_k}$. □

We next prove:

Proposition 4. *Suppose* $(\overline{s_0\ldots s_k})$ *is an allowable sequence with prime period* $k+1$. *Let* $I_s = I_{s_0\ldots s_k s_0\ldots s_k}$ *be a connecting region. Then* F_λ^{k+1} *maps* I_s *two-to-one onto* $I_{s_0\ldots s_k}$, *i.e., there are no critical points in* $F_\lambda^j(I_s)$ *for* $j = 1,\ldots,k-1$.

Proof: Since I_s is a connecting region, the critical point c_{s_0} lies in I_s. Suppose that the critical point in $I_{s_{k-j}}$ lies in the region $I_{s_{k-j}\ldots s_k s_0\ldots s_k}$ for some j with $0 < j < k$. Since the itineraries of c_{s_0} and $c_{s_{k-j}}$ must agree after the second digit, the itinerary of the critical point c_{s_0} must be $s_0 s_1 s_{k-j+2}\ldots s_k s_0\ldots s_k$.

But this itinerary is also $s_0 s_1 \dots s_k s_0 \dots s_k$. Therefore we must have

$$\begin{aligned} s_{k-j+2} &= s_2 \\ s_{k-j+3} &= s_3 \\ &\vdots \\ s_k &= s_j \\ s_0 &= s_{j+1} \\ s_2 &= s_{j+2} \\ &\vdots \end{aligned}$$

It then follows easily that the itinerary $(\overline{s_0 \dots s_k})$ actually has prime period less than $k+1$, which gives a contradiction.

□

In order to invoke the polynomial-like map argument which will produce the accessible Mandelbrot sets, we need to show that F_λ^{k+1} maps the connecting region I_s onto a region that properly contains I_s in its interior. Unfortunately, there are certain allowable sequences for which this is not true. These are the exceptional sequences described in Proposition 2. For example, if $s = (0 \dots 0)$ with $2(k+1)$ zeroes, then it is easy to see that the boundary of $F_\lambda^{k+1}(I_s)$ meets the boundary of $(s_0 \dots s_k) = (0 \dots 0)$ along arcs that lie in the internal rays of angles 0 and $1/4$. Similarly, if $s = (3 \dots 3)$ the boundaries again meet, this time along the internal rays of angles 0 and $3/4$. However, we do not care about these particular sequences, because they do not have prime period $k+1$.

On the other hand, the two collections of symmetrically located connecting regions where $s = (120 \dots 0120 \dots 0)$ and $s = (213 \dots 3213 \dots 3)$ also have this property. We shall deal with these exceptional cases at the end of this section.

First, however, we deal with the non-exceptional cases.

Proposition 5. *Suppose* $(\overline{s_0 \dots s_k})$ *has prime period* $k+1$ *(and is not equal to either* $(\overline{120\dots0})$ *or* $(\overline{213\dots3})$*). Then the connecting regions* $I_{s_0\dots s_k s_0\dots s_k}$ *and* $I_{s_0\dots s_k}$ *have disjoint boundaries.*

Proof: Suppose these two boundaries meet. Applying F_λ^{k+1} to $I_{s_0\dots s_k s_0\dots s_k} \cap I_{s_0\dots s_k}$ yields the set $I_{s_0\dots s_k} \cap F_\lambda(I_{s_k})$. But $F_\lambda(I_{s_k})$ is either $I_0 \cup I_1$ or $I_2 \cup I_3$ depending on s_k, and so the only place where the boundaries could meet would be along the internal rays of angles 0 or 1/2. However, by Proposition 2, the only connectiong regions where this would occur would be $I_{0\dots0}$ and $I_{3\dots3}$ and their symmetrically located images. But we have excluded these cases.

□

It therefore follows from this Proposition that, assuming $(\overline{s_0 \dots s_k})$ is an allowable sequence with prime period $k+1$ (and not one of the exceptional cases) and $I_{s_0\dots s_k s_0\dots s_k}$ is a connecting region, then F_λ^{k+1} is a polynomial-like map of degree two on this disk. By Proposition 3, there exists an open disk $\mathcal{O}$ of parameters for which $F_\lambda(c_{s_0})$ lies in $I_{s_1\dots s_k s_0\dots s_k}$. When $\lambda \in \partial\mathcal{O}$, as shown above, $F_\lambda(c_{s_0})$ lies in the boundary of $I_{s_1\dots s_k s_0\dots s_k}$, and, as λ winds once around $\partial\mathcal{O}$, $F_\lambda(c_{s_0})$ winds once around the boundary of $I_{s_1\dots s_k s_0\dots s_k}$. Moreover, since F_λ^j maps $I_{s_1\dots s_k s_0\dots s_k}$ one-to-one onto $I_{s_j\dots s_k s_0\dots s_k}$, we have that $F_\lambda^j(v_\lambda)$ also winds once around $\partial I_{s_j\dots s_k s_0\dots s_k}$ for each $j \le k$. In particular, $F_\lambda^{k+1}(v_\lambda)$ winds once around the boundary of $I_{s_0\dots s_k}$ as λ winds around the boundary of $\mathcal{O}$. Thus we have shown modulo the exceptional sequences:

Theorem. *Given any allowable sequence* $(\overline{s_0 \dots s_k})$*, there is an open disk of parameters for which* F_λ^{k+1} *is a family of polynomial-like maps of degree two on the connecting region* $I_{s_0\dots s_k s_0\dots s_k}$*.*

By this result, we therefore know that there exists a baby Mandelbrot set in the parameter plane for which the itinerary of the critical point is always

$(\overline{s_0 \dots s_k})$. The question is: is this one of the accessible Mandelbrot sets that extends to the boundary of the connectedness locus in the parameter plane? Since F_λ^{k+1} maps $I_{s_0 \dots s_k s_0 \dots s_k}$ two-to-one over itself, there must be two fixed points (up to multiplicity) for F_λ^{k+1} in this region. One of these fixed points then lies in ∂B_λ since the external ray that corresponds to the itinerary $(\overline{s_0 \dots s_k})$ lands at a periodic point of period $k+1$ in ∂B_λ which then must lie in $I_{s_0 \dots s_k s_0 \dots s_k}$. Consequently, the corresponding quadratic-like Julia sets must extend to the boundary of B_λ. Therefore the corresponding Mandelbrot set is indeed accessible. We thus have:

Corollary. *Given the allowable sequence* $(\overline{s_0 \dots s_k})$*, there exists a baby Mandelbrot set in the parameter plane for* F_λ *for which the cusp of the main cardioid meets* ∂B_λ *at the landing point of the corresponding external ray.*

In Figure 6, we display some of the external rays that land at the cusps of accessible Mandelbrot sets for the family $z^2 + \lambda/z^2$.

We now consider the exceptional case where $s = (120 \dots 0120 \dots 0)$. (The case $(213 \dots 3213 \dots 3)$ may be handled in the same fashion.) We first assume that this sequence is not (1212). In this case the connecting region $I_{120 \dots 0}$ meets the internal ray of angle $1/2$ in an arc γ that connects to ∂T_λ. The smaller connecting region I_s meets this ray in a smaller arc γ' that is contained in γ. So we may extend the connecting region I_s as we did earlier by adding another "rectangular" region that now lies in I_2 and lies slightly below γ'. We may choose this region so that F_λ^{k+1} maps it onto a larger rectangular region that is attached to $I_{120 \dots 0}$ along γ and strictly contains the original smaller rectangular region.

Now, using the H_λ symmetry, we may attach another rectangular region to I_s, this time along the internal ray of angle $1/4$. These are the only two places where the boundaries of I_s and its image under F_λ^{k+1} meet. As before, we call this enlarged connecting region I_s. This region now sits prop-

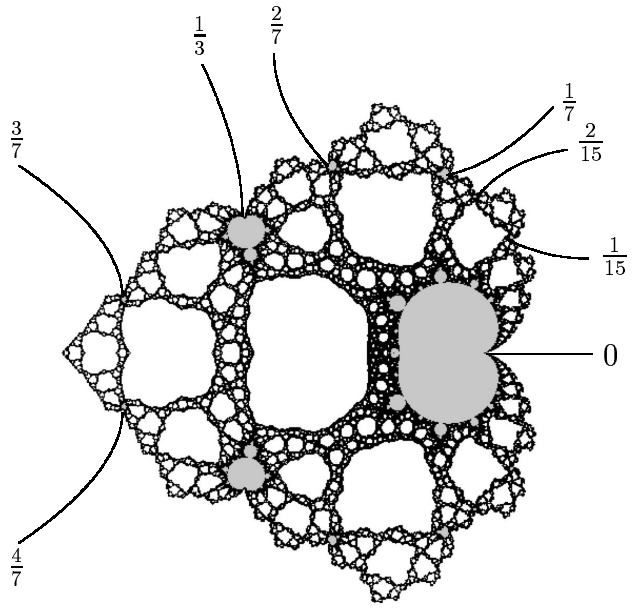

Figure 6: The parameter plane for the family $z^2 + \lambda/z^2$ together with some external rays that land on accessible Mandelbrot sets.

erly inside its image under F_λ^{k+1}, so the polynomial-like map argument used previously now works in this case as well.

When $s = (1212)$, the boundaries of the regions I_s and I_{12} do meet, but not along the internal ray of angle $1/2$. However, proving the existence of a Mandelbrot set with base period 2 in this case is straightforward. Suppose that I_{12} is a connecting region lying in I_1. So, by symmetry, the connecting region in I_2 is I_{20}. Thus there is a non-connecting region I_{21} lying in I_2 that is mapped one-to-one onto I_1. Hence F_λ^2 maps I_{21} two-to-one onto $I_2 \cup I_3 \supset I_{21}$. Also, the critical value of F_λ^2 is just $F_\lambda(c_1)$, so there is an open disk of parameters for which this critical value winds once around the boundary of I_{21} as λ moves around the boundary of this disk. This proves that there is a Mandelbrot set corresponding to the itinerary $(\overline{12})$. A similar argument produces the other base period 2 Mandelbrot set corresponding to the itinerary $(\overline{21})$.

4 Final Comments

In this paper we have concentrated for the most part on the family $z^n + \lambda/z^n$ where $n = 2$. When $n > 2$ the proof of the main result is essentially the same; only a few minor modifications are necessary. For example, in the construction of the internal rays, we used the Cantor necklace that lies in the sectors $S_0 \cup S_2$. When $n > 2$, as described in Section 1, this necklace now lies in $S_0 \cup S_n$. When $n = 2$ we then used two preimages of this necklace at the first stage to generate the internal rays of angles $1/4$ and $3/4$; now we need more preimages to generate the internal rays of angles $j/2n$, but the procedure to do this is exactly the same. Then we continue inductively as before.

Also, the uniformizing map on B_λ now conjugates F_λ on this basin to

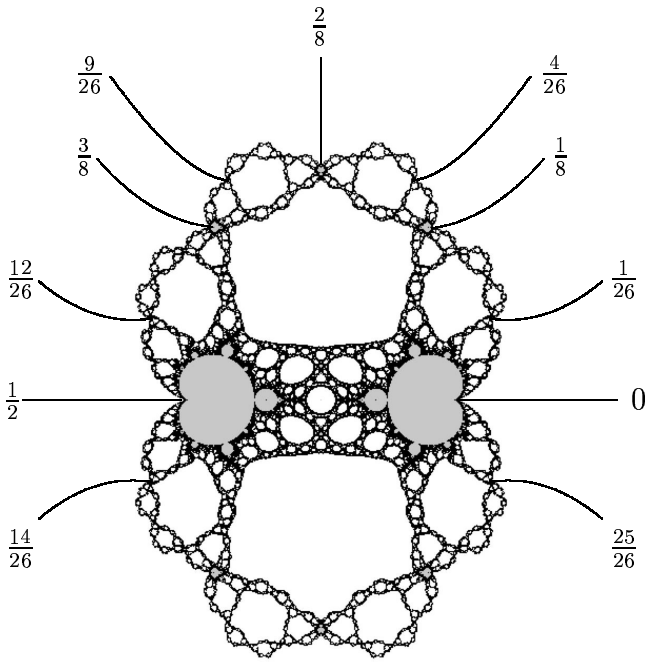

Figure 7: The parameter plane for the family $z^3 + \lambda/z^3$ together with some external rays that land on accessible Mandelbrot sets.

the map $z \mapsto z^n$, so the internal angles (and boundary curves) that are now produced by the earlier construction are of the form j/n^k, while the periodic external rays that land at the cusps of accessible Mandelbrot sets are now of the form $j/(n^k - 1)$. In Figure 7 we display the parameter plane for the case $n = 3$ as well as some of the external rays that land on accessible Mandelbrot sets. In [4], we proved the existence of the $n - 1$ principal Mandelbrot sets that do not appear when $n = 2$.

Finally, recall that, in the case where n is odd, it is not necessarily true that both of the critical values lie on the same critical orbit. However, since there are only two critical values, there can be at most two critical orbits. If there are two such orbits, then they must be symmetric under $z \mapsto -z$, since one orbit contains v_λ and the other $-v_\lambda$. Hence there is one critical point c_j that maps to v_λ in the first orbit (and $n-1$ other critical points map onto v_λ). Then, by symmetry, the other orbit contains $-c_j$ and $-v_\lambda$ (and the other $n - 1$ critical points map onto $-v_\lambda$). Then, assuming that these orbits correspond to allowable repeating sequences, the polynomial-like map argument above applied to either of the corresponding connecting regions produces a single Mandelbrot set associated to such parameters. For each λ in this Mandelbrot set, there are now two distinct and symmetric orbits that behave similarly. For example, in the parameter plane for $n = 3$ (see Figure 7), for λ-values on the positive real line in the main cardioid of the right hand principal Mandelbrot set, there are two distinct attracting fixed points, one lying in $\mathbb{R}^+$, the other in $\mathbb{R}^-$.

The other possibility is that both of the critical values lie on the same critical orbit. These now do not map to the same point as in the case where n is even. Rather, by the $z \mapsto -z$ symmetry, each of these critical values is a distinct point on this orbit. Hence there must be two critical points on this orbit which, by symmetry, must be of the form $\pm c_j$. Then we have

$F_\lambda^k(c_j) = -c_j$ for some k and therefore $F_\lambda^{2k}(c_j) = c_j$. If we were to invoke the polynomial-like mapping argument in such a case, there would then be a problem. If the corresponding allowable sequence is $s = (\overline{s_0 \dots s_{2k-1}})$, then F_λ^{2k} maps I_{ss} four-to-one over itself since F_λ^k maps this connecting region over the region $I_{s_k \dots s_{2k-1} s}$ which contains the other critical point. This would not then yield an actual Mandelbrot set as in the previous cases.

However, we may remedy this as follows. Consider the connecting region $I_{s_0 \dots s_{2k-1} s_0}$ that contains the critical point c_{s_0}. F^k maps this region two-to-one over a different connecting region that contains $-c_{s_0}$, namely $-I_{s_0 \dots s_{k-1} s_0}$. Now consider the map $-F_\lambda^k$ on this region. This now maps $I_{s_0 \dots s_{k-1} s_0}$ two-to-one over itself. Then the polynomial-like mapping argument above produces a Mandelbrot set of base period k for the family $-F_\lambda^k$. But $-F_\lambda^k \circ -F_\lambda^k = F_\lambda^{2k}$, so we would therefore have the same structure in the parameter plane for the map F_λ^{2k} as we do for $-F_\lambda^k$. But this then gives a Mandelbrot set of base period k for F_λ (even though the corresponding attracting periodic orbits have twice this period).

For example, in the left hand principal Mandelbrot set in the case $n = 3$, parameters drawn from the main cardioid now have an attracting cycle of period 2. The corresponding quadratic-like Julia sets are not basilicas in this case; rather, there are two disjoint attracting basins for this cycle, one in the upper half-plane, and the other symmetrically located in the lower half-plane.

References

[1] Blanchard, P., Çilingir, F., Cuzzocreo, D., Devaney, R. L., Look, D. M., and Russell, E. D. Checkerboard Julia Sets for Rational Maps. *International Journal of Bifurcation and Chaos* **23** (2013).

[2] Branner, B. and Fagella, N. *Quasiconformal Surgery in Holomorphic Dynamics.* Cambridge University Press, 2014.

[3] Blanchard, P., Look, D. M., Devaney, R. L., Seal, P., and Shapiro, Y. Sierpinski Curve Julia Sets and Singular Perturbations of Complex Polynomials. *Ergodic Theory and Dynamical Systems* **25** (2005), 1047-1055.

[4] Devaney, R. L. Mandelbrot Sets Adorned with Halos in Families of Rational Maps. In *Complex Dynamics: Twenty-Five Years after the Appearance of the Mandelbrot Set.* American Math Society, Contemporary Math **396** (2006), 37-50.

[5] Devaney, R. L. Intertwined Internal Rays in the Julia Sets of Rational Maps. *Fundamenta Mathematicae* **206** (2009), 139-159.

[6] Devaney, R. L. Cantor Necklaces and Structurally Unstable Sierpinski Curve Julia Sets for Rational Maps. *Qualitative Theory of Dynamical Systems* **5** (2006), 337-359.

[7] Devaney, R. L. Singular Perturbations of Complex Polynomials. *Bulletin of the AMS* **50** (2013), 391-429.

[8] Devaney, R. L. A Cantor-Mandelbrot-Sierpiński Tree in the Parameter Plane for Rational Maps. *Transactions of the AMS* **366** (2014), 1095-1117.

[9] Devaney, R. L. and Look, D. M. Buried Sierpiński Curve Julia Sets. *Discrete and Continuous Dynamical Systems* **13** (2005), 1035-1046.

[10] Devaney, R. L., Look, D. M., and Uminsky, D. The Escape Trichotomy for Singularly Perturbed Rational Maps. *Indiana University Mathematics Journal* **54** (2005), 1621-1634.

[11] Devaney, R. L. and Marotta, S. The McMullen Domain: Rings Around the Boundary. *Transactions of the AMS* **359** (2007), 3251-3273.

[12] Devaney, R. L. and Russell, E. D. Connectivity of Julia Sets for Singularly Perturbed Rational Maps. In *Chaos, CNN, Memristors and Beyond.* World Scientific (2013), 239-245.

[13] Douady, A. and Hubbard, J. Étude Dynamique des Polynômes Complexes. Partie I, *Publ. Math. D'Orsay* **84-02** (1984).

[14] Fitzgibbon, E. and Silvestri, S. Rational Maps: Julia Sets of Accessible Mandelbrot Sets Are Not Homeomorphic. To appear.

[15] McMullen, C. Automorphisms of Rational Maps. *Holomorphic Functions and Moduli*. Vol. 1. Math. Sci. Res. Inst. Publ. **10**. Springer, New York, 1988.

[16] McMullen, C. The Mandelbrot set is universal. In *The Mandelbrot Set, Theme and Variations.* ed. Tan Lei. Cambridge University Press, 2007.

[17] Milnor, J. *Dynamics in One Complex Variable.* Third Edition. Annals of Mathematics Studies. Princeton University Press, (2006).

[18] Petersen, C. and Ryd, G. Convergence of Rational Rays in Parameter Spaces. In The Mandelbrot Set: Theme and Variations. London Math. Soc. Lecture Notes **274**. Cambridge Univ. Press (2000), 161-172.

[19] Qiu, W., Roesch, P., Wang, Z., and Yin, Y. Hyperbolic Components of McMullen Maps. To appear.